ORIGINAL ARTICLE

Feasibility of Smartphone-Based Gait Assessment for Parkinson's Disease

Shih-Tsang Tang[1] · Chun-Hwei Tai[2] · Chia-Yen Yang[1] · Jiun-Hung Lin[3]

Abstract

Purpose There is currently no diagnostic test specific to Parkinson's disease, which means that a positive diagnosis, assessments of severity, and evaluations of treatment efficacy rely heavily on evaluation scales. But obtaining scale data is time-consuming and limited in time and place. Gait is the core target in evaluation scales. Because of the inertia instrument has widely been used in healthcare institutes for gait assessment. Since the inertial device is as well embedded in every smartphone. Our objective was to explore the feasibility of using the ubiquitous smartphone to assist in the assessment of gait.

Methods Twenty subjects were recruited in the clinical trial, which included a general gait analysis and detecting freezing of gait episodes. The gait analysis results obtained using the smartphone were compared with those obtained using an off-the-shelf inertia instrument, and the detecting freezing of gait episodes were compared with the evaluations of clinical professionals.

Results The degree of consistency between the gait analysis results obtained using the smartphone and those obtained using the inertia instrument are $ICC = 0.835$, $r = 0.858$, and $\rho = 0.846$. In the detecting freezing of gait episodes, in comparing the detections by the clinical evaluators and the smartphone, the sensitivity is $90.6 \pm 7.71\%$ and specificity is $94.3 \pm 8.36\%$.

Conclusion The overall analyses revealed high degree of consistency between the two analysis schemes. The convenience of the ubiquitous smartphone has a great potential to enhance the frequency of gait assessment, thereby providing more data by which to assess treatment efficacy.

Keywords Parkinson's disease · Rating scale · Gait analysis · Freezing of gait

1 Introduction

Parkinson's disease (PD) was identified in 1817 by the British physician James Parkinson. PD is a progressive neurological disease involving a gradual deterioration of the substantia nigra cells in the basal ganglia of the brain. The various regions of the brain transmit signals among each other to coordinate the multiple brain functions involved in integrating thoughts, movements, emotions, and feelings. For example, in moving one's body, the basal ganglia sends a message to the thalamus, which is then transmitted to the cerebral cortex and other regions of the brain. The transmission of these messages relies on the neurotransmitter dopamine, which is secreted by the substantia nigra cells. In cases of PD, the deterioration of these cells limits the availability of dopamine for the transmission of nerve signals. Note that the secretion of the neurotransmitter acetylcholine is mediated by dopamine levels. Thus, a decrease in the concentration of dopamine can lead to excessive acetylcholine levels, causing limb tremors and/or muscle rigidity [1].

At present, PD cannot be completely cured; with the result that treatment focuses entirely on the use of drugs or surgical interventions to ease symptoms. Most PD patients suffer from movement disorders, such as bradykinesia, stiffness, tremors, loss of balance, and loss of postural reflexes [2]. PD patients are also susceptible to disruptions in non-motor systems, resulting in micrographia, speech disorders, and/or dysphagia. Furthermore, PD has been linked to mental disorders, sleep disorders, autonomic nerve abnormalities,

✉ Shih-Tsang Tang
    sttang@mail.mcu.edu.tw

1   Department of Biomedical Engineering, Ming-Chuan University, Taoyuan, Taiwan

2   Department of Neurology, National Taiwan University Hospital, Taipei, Taiwan

3   Department of Electronic Engineering, Kun Shan University, Tainan, Taiwan

paresthesia, and gastrointestinal discomfort [3]. Aging, genetic factors and exposure to pesticides or industrial waste have also been shown to accelerate PD-related deterioration [4].

In today's aging society, PD and dementia are the most common chronic neurodegenerative diseases. PD morbidity is approximately 0.1–0.2%; however, the onset of PD increases sharply with age, especially after 60 years old. The number of PD onset events per 100,000 people per year ranges from 17.4 (50–59 years) to 93.1 (70–79 years). The prevalence of PD among those over the age of 60 is approximately 1.5% [5, 6], and it has been estimated that 15% of the population over the age of 65 is affected. Note that the onset of PD can occur even before the age of 40. Currently, there are roughly 500,000 cases of PD in Europe and one million cases in the United States, with an annual growth rate of 50,000–60,000. The average life expectancy from diagnosis to death is 15 years, and mortality is more than double that in the general population [7]. As a progressive disease, PD gradually degrades one's quality of life, because patients lose the ability to look after themselves or speak with others. By the time they reach the final stage of the disease, most PD patients are unable to eat due to dysphagia, which can result in severe weakness and concurrent aspiration pneumonia. PD brings with it a long period of pain and suffering for patients as well as their families.

At present, there are no diagnostic tests (e.g., blood, urine, imaging, or physiological signals) specifically for PD. In the initial stages, PD is diagnosed via clinical examination. Typical symptoms include bradykinesia, akinesia, resting tremors, and rigidity [8]. Postural abnormality is another common symptom, which tends to appear in later stages. Note, however, that many PD patients are asymptomatic; i.e., they do not exhibit tremors. A clinical diagnosis of PD is evidence of at least two of the above-mentioned symptoms. Subsequent confirmation is based on the effectiveness of PD drug therapy. A variety of scales have been developed for the rating of PD symptoms. Some scales are used in research for the evaluation of treatment efficacy, whereas others are used clinically to assess disease progression and severity [9]. The Hoehn-Yahr scale and Unified Parkinson's Disease Rating Scale (UPDRS) are used most commonly today. The Hoehn-Yahr scale is used to stage the course of PD [10], and the UPDRS is used to evaluate treatment efficacy [11]. In the initial stages (the first 10–15 years), PD patients are treated with drugs to relieve symptoms. The most common drug is levodopa, which is meant to supplement dopamine loss [4]. However, the efficacy of drugs diminishes over time, such that surgical interventions, such as deep brain stimulation (DBS) and brain lesioning, would be considered.

Dyskinesia is the main symptom of PD, and gait is the most representative item. Gait assessment can be used to screen patients with suspected PD and can also be used to monitor disease progression and evaluate the treatment efficacy. Thus, gait is the main evaluation topic on the UPDRS and the Hoehn-Yahr scale. Deep brain stimulation surgery is expensive and high-risk, and until recently, there has been no effective method by which to predict the prognosis. Recent studies however, have revealed that gait assessment can be used to predict DBS prognosis [12]. Nonetheless, gait assessment must be performed by trained clinical professionals, which is time-consuming, and is limited in time and place. As a result, the insufficient assessment is the general situation.

Microelectromechanical inertia instrument has widely been used in healthcare institutes for gait assessment [13–15]. Because of the inertial device is as well embedded in every smartphone. Our objective in the current study was to explore the feasibility of using a smartphone to assist in the assessment of gait in cases of PD. The ubiquity of smartphones should make it possible to perform regular gait assessments to keep track of disease progression and the efficacy of treatment.

2 Methods

PD gait assessment can be divided into general gait analysis and detecting freezing of gait (FoG) episodes. This section outlines gait assessment methods, experimental tools, and clinical trials.

2.1 General Gait Analysis

Figure 1 outlines the flow of signal data processing for general gait analysis using the inertial device embedded in smartphones to measure vertical acceleration along the sagittal plane during walking. Imported raw acceleration data first undergo signal pre-processing, which involves filtering out environmental noise and deleting signals corresponding to the start and end of the walking segment. Filtering is also performed to remove interference due to acceleration under the effects of
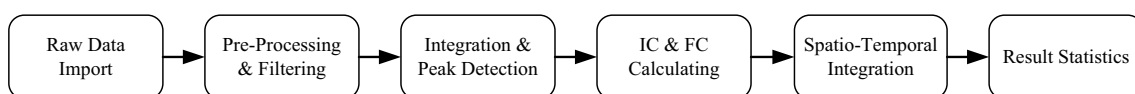

Fig. 1 The process of the general gait analysis

gravity. Signal smoothing is then used to facilitate the detection of peaks. The Gaussian Continuous Wavelet Transform (GCWT) is applied to the signal, such that the valley of the resulting waveform corresponds to the time point of the initial contact (IC) of the foot (i.e., the point at which the heel strikes the ground). The GCWT is then applied again, the peak of the resulting waveform corresponding to the time point of the final contact (FC) of the foot (i.e., the point at which the toes leave the ground). Spatio-temporal integration is then used to determine the spatial positions corresponding to the time points of IC and FC [14, 15].

Once the IC and FC have been identified, it is possible to analyze gait features, including pace, rhythm, variability, asymmetry, and postural control. Gait pace includes step velocity mean, step length mean, and swing time variability. Gait rhythm includes step time mean, swing time mean, and stance time mean. Gait variability includes step velocity variability, step length variability, step time variability, and stance time variability. Gait asymmetry includes swing time asymmetry, step time asymmetry, and stance time asymmetry. Postural control includes step length asymmetry, step width mean, and step width variability. The structure of general gait analysis is shown in Fig. 2.

For a compass gait type, the center of mass (CoM) movements in the sagittal plane follow a circular trajectory during each single support phase. Then in the inverted pendulum model, the variations in height of CoM depend on step length [16]. Thus, the step length could be derived using the elevation (and variation in elevation) of the inertial device from the ground [17], as follows:

$$Step\ Length = 2 \cdot \sqrt{2lh - h^2} \tag{1}$$

where l indicates the elevation of the inertial device above the ground (pendulum length) while the subject is standing still, and h indicates the variability in elevation while the subject is walking. The h is calculated by a double integration of vertical acceleration. To prevent integration drift, data were high-pass filtered in advance.

The step velocity is derived using step length and step time, as follows:

$$Step\ Velocity = \frac{Step\ Length}{Step\ Time} \tag{2}$$

The degree of variability of the right and left foot data are derived from the variance of the right foot and left foot, as follows:

$$Variability_{left\ and\ right} = \sqrt{\frac{Variance_{left} - Variance_{right}}{2}} \tag{3}$$

where $Variability_{left\ and\ right}$ refers to the variation of the left foot and right foot, $Variance_{left}$ refers the variance of the left foot, and $Variance_{right}$ refers to the variance of right foot.

Variability in gait features is derived from the standard deviation (SD) in data pertaining to walking, for example,

$$Variability = SD(Steps) \tag{4}$$

Symmetry between the left foot and right foot is derived from the averages of the left foot and right foot, for example,

$$Asymmetry_{left\ and\ right} = |Average_{left} - Average_{right}| \tag{5}$$

where $Asymmetry_{left\ and\ right}$ refers to the absolute difference between the averages of the left foot $Average_{left}$ and the right foot $Average_{right}$.

Figure 3 presents a schematic illustration showing the derivation of gait analysis results, where the blue wave indicates raw walking data; the green wave is derived from the initial GCWT (following data integration and smoothing)
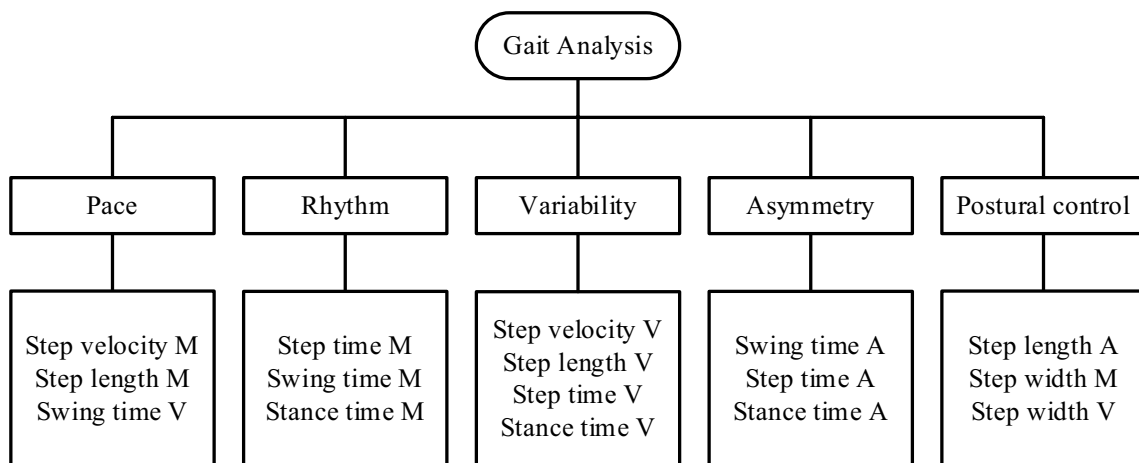

Fig. 2 Structure of general gait analysis, where M refers to mean, A refers to asymmetry, and V refers to variability
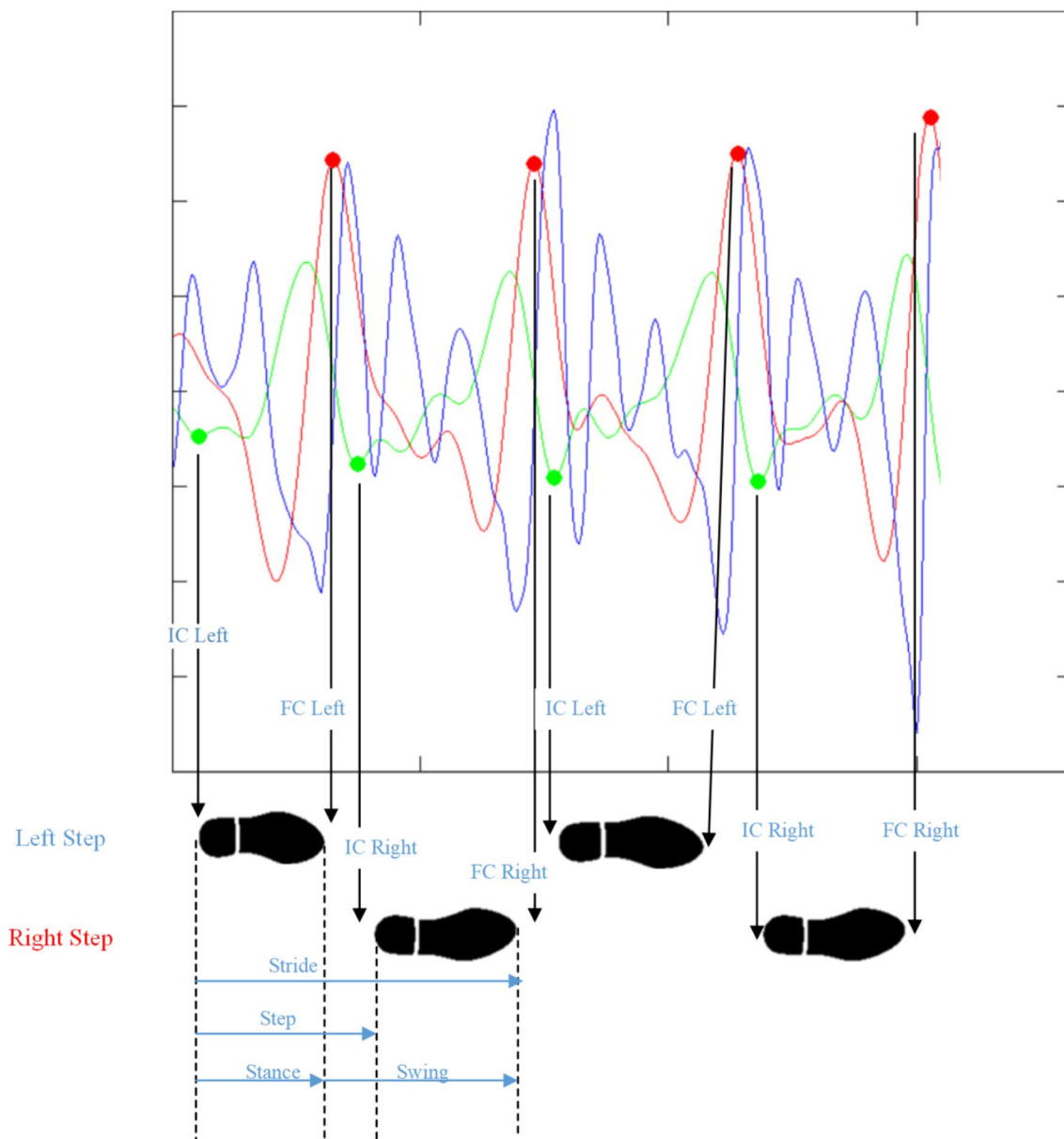
Fig. 3 Schematic illustration showing the derivation of gait analysis results

with the valley corresponding to the IC time point; and the red wave is derived from the second GCWT with the peak corresponding to the FC time point. The IC and FC time points of the left foot and right foot are differentiated by the sign of angular velocity along the vertical axis after filtering.

2.2 FoG Detection

When PD patients stand or walk normally, the power spectrum of vertical acceleration along the sagittal plane is distributed mainly in the loco band (0.5–3 Hz). FoG episodes produce a significant spectral component referred to as the freeze band (3–8 Hz) [15, 18]. A FoG episode can be detected using a 256-point Hamming sliding window for the filtering of vertical acceleration data with a data shift of 40 points per slide movement. Data captured from each window data undergo processing via fast Fourier transform (FFT) to calculate the power spectral density (PSD). Trapezoidal integration is then performed respectively on the freeze band and the loco band. The sum of the integration results of the two frequency bands are referred to as the energy index (EI) [15], and the integration of the freeze band divided by the integration of the loco band is referred to as the freezing index (FI). Freezing threshold FI_{th} and energy threshold EI_{th} are used to determine the occurrence of FoG episodes. FI_{th} and EI_{th} vary from person to person and must therefore be

obtained via practical testing. Step cadence (*SC*) is determined from the second harmonic in the spectrum. Human gait is a periodic phenomenon, and the number of steps per unit time is the second harmonic in the walking spectrum [19]. The process of FoG episode detection is illustrated in Fig. 4.

The following criteria are used to detect FoG episodes:

$$Criterion\ 1 \equiv \left(FI(i) > FI_{th} \right) \wedge \left(EI(i) > EI_{th} \right) \quad (6)$$

$$Criterion\ 2 \equiv (SC(i) \neq SC(i-1)) \wedge (SC(i-1) \neq SC(i-2)) \quad (7)$$

$$Criterion\ 3 \equiv (SC(i) \geq SC(i-1)) \wedge (SC(i-1) > SC(i-2)) \quad (8)$$

where $\wedge$ is the AND logical operator. When $FI(i)$ and $EI(i)$ of the i_{th} data window both exceed the critical values FI_{th} and EI_{th}, then *Criterion* 1 is true. When the *SC* of three consecutive window frames $(i-2, i-1, i)$ are not equal, *Criterion* 2 is true. A progressive increase in the *SC* of three consecutive window frames $(i-2, i-1, i)$ indicates an increase in the walking steps, such that *Criterion* 3 is true. The FoG episode begins at

$$Criterion\ 1 \wedge (Criterion\ 2 \vee Criterion\ 3) = Truth \quad (9)$$

where $\vee$ is the OR logical operator. The FoG episode ends at

$$Criterion\ 1 \vee (Criterion\ 2 \wedge Criterion\ 3) = False \quad (10)$$

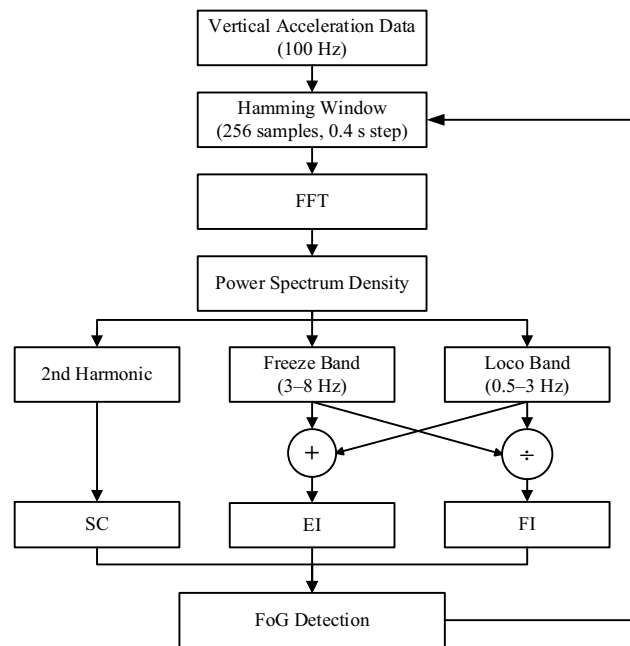The PSD of a FoG episode is shown in Fig. 5, the PSD of normal walking is shown in Fig. 6, the PSD of standing still is shown in Fig. 7, and the accumulation of the aforementioned three PSDs is shown in Fig. 8. Most of the energy of FoG episodes and normal walking is distributed in the range of 0–40 Hz. Standing still implies little or no movement; therefore, most of the PSD can be attributed to noise with most of the energy distributed below 0.5 Hz. Note also that the total energy involved in standing still is significantly lower than that of FoG episodes and normal walking. The cumulative PSD can be used to distinguish instances of standing still, where FI_{th} and EI_{th} are the average values plus the standard deviation estimated for a subject standing still for 20 s.
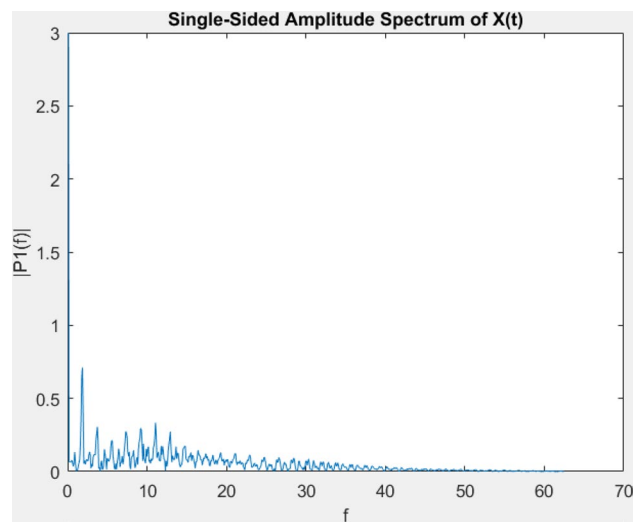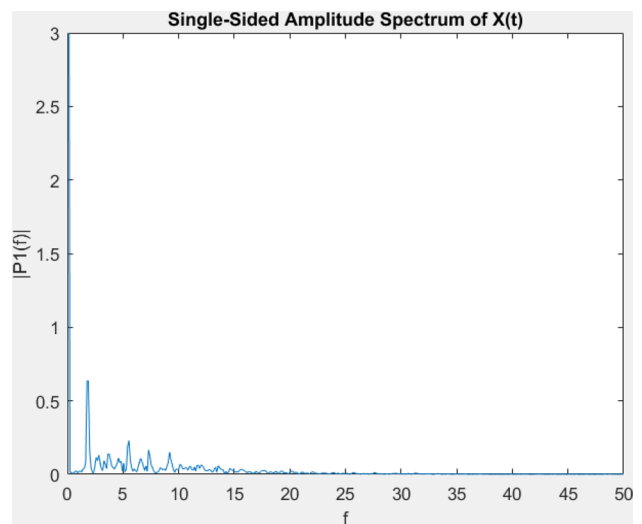

Fig. 5 PSD of FoG episode

Fig. 6 PSD of normal walking

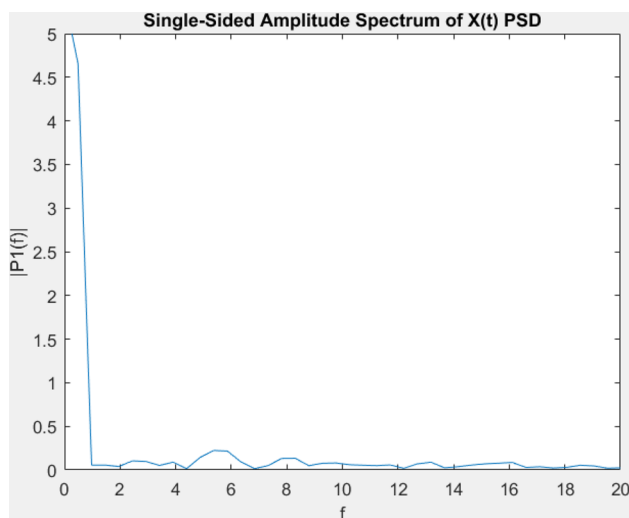**Fig. 4** Process used in FoG episode detection
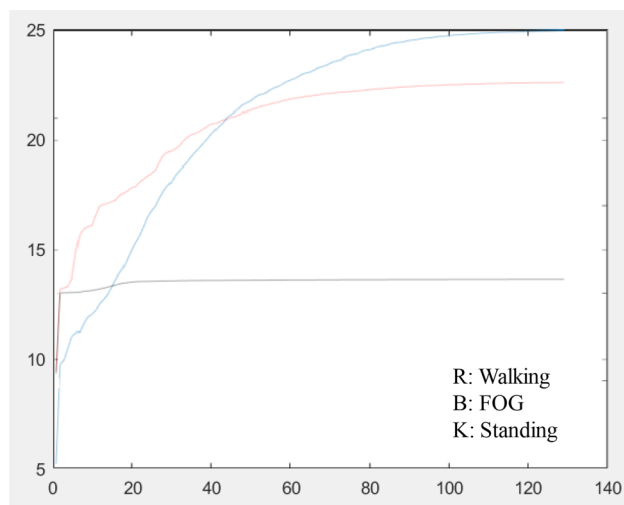
Fig. 7 PSD of standing still

Fig. 8 Accumulated PSD of FoG episode, normal walking, and standing still

2.3 Experimental Tools

This study requires a smartphone that is small, light, and computationally powerful. The following experiments were performed using a Sony™ Xperia XZ F8331 ($146 \times 72 \times 8.1$ mm; 161 g) with a powerful quad-core processor (2×2.15 GHz Kryo and 2×1.6 GHz Kryo), the Qualcomm MSM8996 Snapdragon 820 chipset, an Adreno 530 graphics processor, and 3 GB RAM/ 32 GB ROM. The operating system was Android 8.0 (Oreo). Note that this smartphone also features a solid aluminum back and frame shell with a wear-resistant Corning Gorilla Glass 4 screen. The embedded inertial device is the Bosch BMI160 MEMs chip, comprising a 16-bit three-axis accelerometer

and three-axis gyroscope. The sensing range of the accelerometer is ± 2 g, ± 4 g, ± 8 g, and ± 16 g. The sensing range of the gyroscope is $\pm 125°/s$, $\pm 250°/s$, $\pm 500°/s$, $\pm 1000°/s$, and $\pm 2000°/s$.

The gait analysis results obtained using the smartphone were compared with those obtained using an XsensTM MTw Awinda, which is widely applied in clinical experiments. FoG detection results were evaluated by clinical professionals, who sought to identify FoG episodes by examining video segments from the same analysis sessions.

2.4 Clinical Trials

The sample size of this trial ($n = 20$) was in line with the recommendations of the Lee Silverman Voice Treatment [20, 21]. In this study, type-I error α was set to 0.05, statistical power was set to 80%, and the withdrawal rate was estimated at 20%.

The criteria for the inclusion of subjects were as follows:

1. Over 20 years old (legal age),
2. Typical PD patient,
3. In 2−4 PD Hoehn-Yahr stages,
4. Ability to walk independently (i.e., without assistance from others),
5. No comorbidity of mental or intellectual impairment (i.e., ability to understand instructions during the trial).

The criteria for the exclusion of subjects were as follows:

1. Atypical PD patient,
2. Impaired intelligence, confusion, depression, and/or loss of motivation,
3. Acute illness or disease of the central or peripheral nervous system, which could potentially affect walking,
4. Orthopedic or internal medical problems potentially affecting walking,
5. Vulnerable groups, such as prisoners, indigenous people, pregnant women, or mental patients.

Throughout the experiment, an elastic band was used to fix both the MTw Awinda and the smartphone adjacent to the center of the body mass, which is behind the navel against the second lumbar spine (L2). Participants performed a timed up and go test (TUG), which involved walking in a straight line and then turning back. Note that from the perspective of signal processing, this routine would produce large fluctuations in velocity at the starting and ending points. Thus, we extended the walking distance (normally 3 m) to 5 m, with the aim of ensuring stable velocity for a sufficient duration, as shown in Fig. 9. During the FoG episode detection test, FoG episodes were induced by placing additional obstacles on the walking pathway.
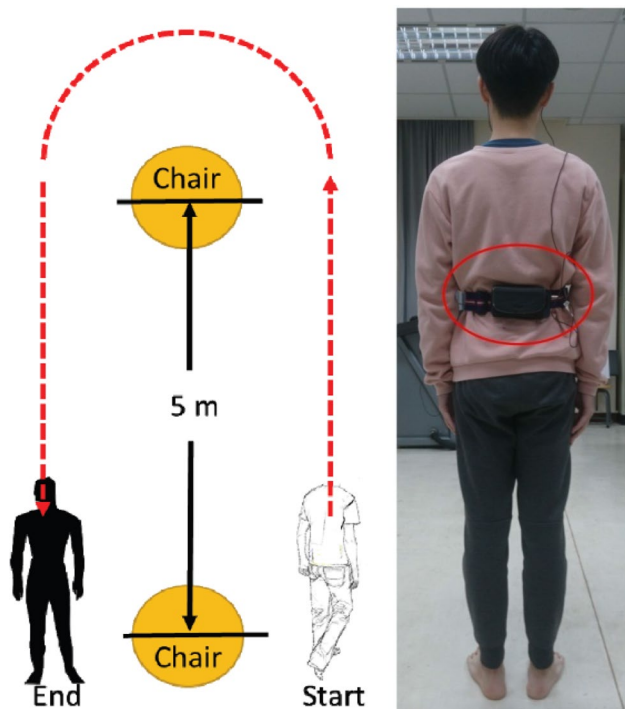
Fig. 9 Illustration of walking pathway and positioning of smartphone and MTw Awinda (Red circle)

Table 1 Demographic background information of study subjects

Age (year)	73.6 (54−86)
Gender	9 female, 11 male
PD course (year)	15.3 (4−25)
FoG course (year)	8.7 (6−11)
Hoehn-Yahr Stage	3.2 (2−4)
MDS-UPDRS-part III	40.6 (10−69)
N-FOGQ	17.6 (9−27)
MMSE	26.5 (25−30)

3 Results

The clinical trial was approved by the Clinical Trial Center, National Taiwan University Hospital, and all subjects provided written informed consent. As shown in Table 1, the demographic background information of the subjects included age, gender, duration of suffering from PD, duration of FoG occurrence, Hoehn-Yahr stage, evaluation of the UPDRS part III, evaluation of the New Freezing of Gait Questionnaire (N-FOGQ), and evaluation of Mini-Mental State Examination (MMSE).

The gait analysis items used to compare the performance of the proposed smartphone and the MTw Awinda were as follows: step count, step time, stride time, stance time, swing time, step length, and step velocity. The measured number of steps obtained using the smartphone was 100% consistent with the results from the MTw Awinda. After verifying the normal distribution of results from the Shapiro–Wilk test, the experiment data were analyzed in terms of level of agreement (LoA): mean, standard deviation, intraclass correlation coefficient (ICC), correlation coefficient analysis (r), Spearman correlation coefficient analysis (ρ), and $\pm 95\%$ confidence interval analysis, as shown in Table 2.

Independent t-test tests and analysis of variance (ANOVA) were used to analyze the between-group differences. The relatively small number of subjects limited the effects of data reorganization; therefore, Bonferroni correction was not performed [22]. In accordance with the recommendations of Hartmann and Portney [23, 24], the degree of consistency was defined in terms of ICC, r, or ρ, as follows: excellent (> 0.900), good ($0.750−0.899$), medium ($0.500−0.749$), and inconsistent (< 0.500). The results in Table 2 illustrate the high degree of consistency between the gait analysis result obtained using the smartphone and those obtained using the MTw Awinda. The averages of ICC, r, and ρ are 0.835, 0.858, and 0.846, respectively. Figure 10 compares the time-series of step counts obtained using the MTw Awinda and the smartphone.

The detection of FoG episodes depends on two types of movement disorders: akinetic and tremoric. Note that at least one FoG episode was identified during the test session of each subject, and a total of 39 FoG episodes (#FoG) were identified among all subjects. Note also that three evaluators with clinical experience participated in the analysis, and their results presented high inter-rater agreement. There was a clear consensus with regard to the time points corresponding to the start and end of the FoG episodes ($ICC > 0.82$). The smartphone detected only 35 #FoG (89.7%). The detection sensitivity and specificity of the clinical evaluators and smartphone were respectively derived as follows:

$$Sensitivity = \frac{Phone\ FRs}{Clinic\ FRs} \times \frac{100}{100} \quad (11)$$

$$Specificity = \frac{Phone\ NFRs}{Clinic\ NFRs} \times \frac{100}{100} \quad (12)$$

where *Phone FRs* indicates the #FoG detected by the smartphone, *Clinic FRs* indicates the #FoG identified by clinical evaluators, and *NFRs* refer to non-FoG periods. The analysis results are detailed in Table 3. We also compared the measurements obtained by the evaluators and the smartphone. The average times were as follows: evaluators (6.50 ± 2.36 s.) and smartphone (6.20 ± 2.40 s.). The consistency between the

Table 2 Consistency analysis: results obtained using smartphone and MTw Awinda

|	Mean ± SD		Levels of Agreement			
	MTw Awinda	Smartphone	ICC	r	ρ	$\bar{x} \pm 95\%$
Mean						
Stride time (s)	1.04 ± 0.036	1.03 ± 0.044	0.832	0.847	0.772	0.021 ± 0.00462
Step time (s)	0.526 ± 0.022	0.523 ± 0.027	0.801	0.819	0.846	0.00319 ± 0.0138
Stance time (s)	0.666 ± 0.026	0.675 ± 0.0360	0.811	0.886	0.798	0.0169 ± 0.00451
Swing time (s)	0.374 ± 0.019	0.377 ± 0.023	0.836	0.855	0.827	0.0081 ± 0.00397
Step length (cm)	65.1 ± 2.74	65.8 ± 2.57	0.874	0.905	0.876	1.12 ± 0.337
Step velocity (cm/s)	124 ± 7.53	127 ± 11.2	0.822	0.820	0.808	6.17 ± 1.64
Variability						
Stride time (s)	0.0236 ± 0.004	0.0256 ± 0.005	0.768	0.887	0.802	0.00261 ± 0.000593
Step time (s)	0.0221 ± 0.015	0.0233 ± 0.011	0.809	0.813	0.814	0.00543 ± 0.00179
Stance time (s)	0.0199 ± 0.006	0.0204 ± 0.007	0.896	0.914	0.893	0.00247 ± 0.000742
Swing time (s)	0.0161 ± 0.006	0.0155 ± 0.008	0.820	0.844	0.865	0.00343 ± 0.00105
Step length (cm)	4.06 ± 1.78	4.48 ± 2.40	0.827	0.875	0.898	0.963 ± 0.359
Step velocity (cm/s)	10.3 ± 4.10	10.9 ± 5.54	0.829	0.864	0.905	2.41 ± 0.682
Asymmetry						
Stride time (s)	0.0812 ± 0.049	0.0823 ± 0.050	0.874	0.869	0.835	0.0213 ± 0.00579
Step time (s)	0.0598 ± 0.036	0.0567 ± 0.0380	0.826	0.823	0.865	0.01751 ± 0.00591
Stance time (s)	0.0637 ± 0.040	0.0549 ± 0.036	0.849	0.869	0.874	0.0156 ± 0.00644
Swing time (s)	0.0332 ± 0.021	0.0344 ± 0.023	0.86	0.861	0.831	0.00937 ± 0.00309
Step length (cm)	1.53 ± 0.890	1.58 ± 1.01	0.836	0.836	0.802	0.421 ± 0.153
Step velocity (cm/s)	13.9 ± 8.78	14.5 ± 9.66	0.859	0.858	0.920	3.43 ± 1.57
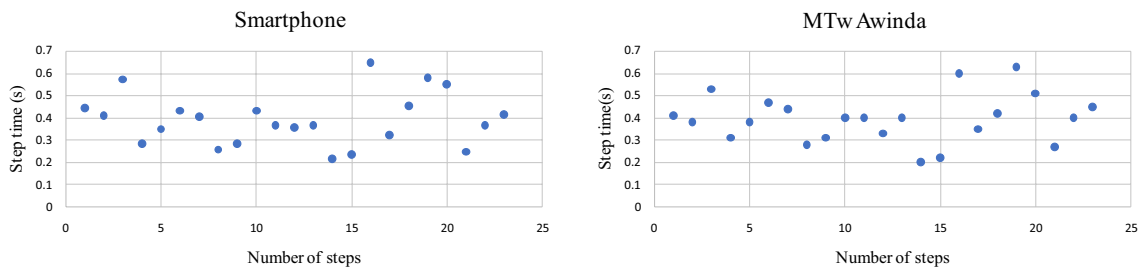
Fig. 10 Time series of step counts obtained using smartphone and MTw Awinda

two data sets was as follows: $ICC = 0.972$, $r = 0.971$, and $\rho = 0.947$. Overall, the above analysis revealed outstanding consistency between the two analysis schemes.

4 Discussion

The primary differences between the smartphone and the MTw Awinda are the sampling rate and tasking mode of the kernel processor. It is possible to set the sampling rate of the inertial device embedded in a smartphone to match that of the MTw Awinda; however, the MTw Awinda operates in single tasking mode, while the smartphone operates in multitasking mode. This allows the MTw Awinda to maintain a constant sampling rate and frequency resolution

while calculating the gait spectrum. The system resources of smartphones are controlled by the Android operating system, in which background programs share resources and priority is given to programs that are responsible for core tasks, such as the real-time clock and phone standby. Thus, smartphones cannot ensure that sampling of the embedded inertial device proceeds at a constant rate. These fluctuations can have a direct effect on the spectral resolution, which is crucial to determining the occurrence of FoG episodes. This problem could be alleviated by using a more powerful processor or reducing the number of programs running in the background. In this study, we initially assessed the Sony™ Xperia and Samsung™ Galaxy smartphones, both of which feature quad-core processors. We then discovered that the Galaxy tends to

Table 3 FoG episode detection: sensitivity and specificity

	Gender	Age (year)	Type	#FoG	Sensitivity	Specificity
Subject 1	Male	86	Akinetic	3	90.7%	100.0%
Subject 2	Male	72	Akinetic	2	90.9%	91.5%
Subject 3	Female	66	Tremoric	1	94.7%	100.0%
Subject 4	Male	83	Tremoric	1	86.2%	99.7%
Subject 5	Female	66	Akinetic	2	77.0%	100.0%
Subject 6	Male	70	Tremoric	1	100.0%	65.8%
Subject 7	Male	65	Akinetic	2	89.7%	92.1%
Subject 8	Female	82	Akinetic	2	76.3%	97.4%
Subject 9	Male	76	Akinetic	3	96.0%	84.3%
Subject 10	Male	84	Tremoric	2	91.8%	95.5%
Subject 11	Female	77	Akinetic	2	87.1%	97.5%
Subject 12	Male	54	Tremoric	1	100.0%	91.1%
Subject 13	Female	69	Akinetic	2	93.2%	83.5%
Subject 14	Male	76	Akinetic	3	78.5%	94.5%
Subject 15	Male	82	Akinetic	2	100.0%	96.6%
Subject 16	Female	79	Tremoric	2	90.7%	100.0%
Subject 17	Female	84	Akinetic	2	98.6%	99.1%
Subject 18	Female	56	Tremoric	1	99.9%	100.0%
Subject 19	Female	70	Tremoric	2	81.1%	98.2%
Subject 20	Male	74	Akinetic	3	89.9%	98.5%
				39	$90.6 \pm 7.71\%$	$94.3 \pm 8.36\%$

have a larger number of proprietary apps running in the background and sharing more system resources; therefore, we opted for the Sony device in the above experiments. Gait detection performance could also be improved by reducing the computational load on the smartphone. In the above experiments, we sought to optimize measurement performance by restoring the phone to its factory settings, deleting all pre-installed apps, and closing all built-in apps, such as GPS and synchronizer. The resulting measurement results did not differ significantly from those obtained from the MTw Awinda; however, it is unlikely that the same benchmarks could be achieved using a typically configured smartphone.

It should also be noted that the clinical evaluators would be able to use their extensive experience in interpreting the body language of subjects, such as facial expressions and body movements. In contrast, smartphones depend entirely on objective variations in gait, while disregarding FoG episodes of short duration and underestimating the duration of FoG episodes. As a result, clinical evaluators tend to be more sensitive than is smartphone.

The results of this experiment revealed that most of the situations involving FoG episodes occurred during changes in routine (e.g., walking initiation, turning, approaching the ending point, or passing through the midway obstacles), which is in line with general clinical symptoms. We also found that the symptoms (akinetic, tremoric), FoG forms (trembling, shuffling, akinetic), Hoehn and Yahr stages, or

gender did not diverge from the measurements obtained using the smartphone or the MTw Awinda.

Finally, it should be noted that our focus in this study was on engineering issues. The role of gait assessment in clinical diagnosis has not been fully elucidated. The means by which gait analysis (e.g., FoG detection and its duration) contribute to clinical diagnosis and the degree of accuracy required for this analysis will have to be examined in the future.

The system developed in this study could greatly enhance the convenience and frequency of PD gait assessment, thereby providing more data by which to assess treatment efficacy.

References

1. Latash, M. L. (2008). *Postural control and locomotion in Parkinson's disease. Neurophysiological basis of movement* (pp. 325–326). Illinois: Champaign.
2. Lees, A. J., Hardy, J., & Revesz, T. (2009). Parkinson's disease. *Lancet, 373*(9680), 2055–2066. https://doi.org/10.1016/S0140 -6736(09)60492-X.
3. Chaudhuri, K. R., & Schapira, A. H. (2009). Non-motor symptoms of Parkinson's disease: Dopaminergic pathophysiology and treatment. *Lancet Neurology, 8*(5), 464–474. https://doi.org/10.1016/ S1474-4422(09)70068-7.

4. Environmental Factors and Parkinson's. *National Parkinson Foundation*. Retrieved from https://www.parkinson.org/understanding-parkinsons/what-is-parkinsons/Environmental-Factors-and-Parkinsons

5. Bower, J. H., Maraganore, D. M., McDonnell, S. D. K., & Rocca, W. A. (1999). Incidence and distribution of parkinsonism in Olmsted County, Minnesota, 1976–1990. *Neurology, 52*(6), 1214–1220.

6. de Rijk, M. C., Breteler, M. M., Graveland, G. A., Ott, A., Grobbee, D. E., van der Meché, F. G., et al. (1995). Prevalence of Parkinson's disease in the elderly: the Rotterdam Study. *Neurology, 45*(12), 2143–2146.

7. Katzenschlager, R., Head, J., Schraq, A., Ben-Shlomo, Y., Evans, A., & Lees, A. J. (2008). Fourteen-year final report of the randomized PDRG-UK trial comparing three initial treatments in PD. *Neurology, 71*(7), 474–480.

8. Jankovic, J. (2008). Parkinson's disease: Clinical features and diagnosis. *Journal of Neurology, Neurosurgery and Psychiatry, 79*(4), 368–376. https://doi.org/10.1136/jnnp.2007.131045.

9. Professional Training. *National Parkinson Foundation*. Retrieved from https://www.parkinson.org/Professionals/Professional-Resources/Screening-Instruments

10. Goetz, C. G., Poewe, W., Rascol, O., Sampaio, C., Stebbins, G. T., Counsell, C., et al. (2004). Movement disorder society task force report on the Hoehn and Yahr staging scale: Status and recommendations. *Movement Disorders, 19*(9), 1020–1028.

11. Goetz, C. G., Tilley, B. C., Shaftman, S. R., Stebbins, G. T., Fahn, S., Martinez-Martin, P., et al. (2008). Movement disorder society-sponsored revision of the unified Parkinson's disease rating scale (MDS-UPDRS): Scale presentation and clinimetric testing results. *Movement Disorders, 23*(15), 2129–2170.

12. Lilleeng, B., Gjerstad, M., Baardsen, R., Dalen, I., & Larsen, J. P. (2015). Motor symptoms after deep brain stimulation of the subthalamic nucleus. *Acta Neurologica Scandinavica, 131*(5), 298–304. https://doi.org/10.1111/ane.12342.

13. Del Din, S., Godfrey, A., & Rochester, L. (2015). Validation of an accelerometer to quantify a comprehensive battery of gait characteristics in healthy older adults and Parkinson's disease: Toward clinical and at home use. *IEEE Journal of Biomedical and Health Informatics, 20*(3), 838–847. https://doi.org/10.1109/JBHI.2015.2419317.

14. Godfrey, A., Lara, J., Munro, C. A., Wiuff, C., Chowdhury, S. A., Del Din, S., et al. (2015). Instrumented assessment of test battery for physical capability using an accelerometer: A feasibility study. *Physiological Measurement, 36*(5), N71–83.

15. Moore, S. T., MacDougall, H. G., & Ondo, W. G. (2008). Ambulatory monitoring of freezing of gait in Parkinson's disease. *Journal of Neuroscience Methods, 167*(2), 340–348.

16. Zijlstra, W., & Hof, A. (1997). Displacement of the pelvis during human walking: Experimental data and model predictions. *Gait & Posture, 6*(3), 249–262. https://doi.org/10.1016/s0966-6362(97)00021-0.

17. Zijlstra, W., & Hof, A. L. (2003). Assessment of spatio-temporal gait parameters from trunk accelerations during human walking. *Gait & Posture, 18*(2), 1–10. https://doi.org/10.1016/s0966-6362(02)00190-x.

18. Auvinet, B., Berrut, G., Touzard, C., Moutel, L., Collet, N., Chaleil, D., et al. (2002). Reference data for normal subjects obtained with an accelerometric device. *Gait Posture, 16*(2), 124–134.

19. Moore, S. T., Yungher, D. A., Morris, T. R., Dilda, V., MacDougall, H. G., Shine, J. M., et al. (2013). Autonomous identification of freezing of gait in Parkinson's disease from lower-body segmental accelerometry. *Journal of NeuroEngineering and Rehabilitation, 10*, 19. https://doi.org/10.1186/1743-0003-10-19.

20. Ramig, L. O., Countryman, S., O'Brien, C., Hoehn, M., & Thompson, L. (1996). Intensive speech treatment for patients with Parkinson's disease: Short-and long-term comparison of two techniques. *Neurology, 47*(6), 1496–1504.

21. Ramig, L. O., Countryman, S., Thompson, L. L., & Horii, Y. (1995). Comparison of two forms of intensive speech treatment for Parkinson disease. *Journal of Speech and Hearing Research, 38*(6), 1232–1251.

22. Armstrong, R. A. (2014). When to use the Bonferroni correction. *Ophthalmic and Physiological Optics, 34*(5), 502–508. https://doi.org/10.1111/opo.12131.

23. Hartmann, A., Luzi, S., Murer, K., de Bie, R. A., & de Bruin, E. D. (2009). Concurrent validity of a trunk tri-axial accelerometer system for gait analysis in older adults. *Gait & Posture, 29*(3), 444–448. https://doi.org/10.1016/j.gaitpost.2008.11.003.

24. Portney, L. G., & Watkins, M. P. (2015). *Foundations of clinical research: Applications to practice*. Pennsylvania: F.A. Davis Company.